6268–6279 *Nucleic Acids Research, 2007, Vol. 35, No. 18* *Published online 13 September 2007*
doi:10.1093/nar/gkm691

Deletion of the nuclear exosome component RRP6 leads to continued accumulation of the histone mRNA HTB1 in S-phase of the cell cycle in *Saccharomyces cerevisiae*

Ruth Canavan and Ursula Bond*

Department of Microbiology, Moyne Institute for Preventive Medicine, Trinity College, University of Dublin, Dublin, Ireland

Received March 9, 2007; Revised and Accepted August 22, 2007

ABSTRACT

The nuclear exosome, a macromolecular complex of 3′ to 5′ exonucleases, is required for the post-transcriptional processing of a variety of RNAs including rRNAs and snoRNAs. Additionally, this complex forms part of a nuclear surveillance network where it acts to degrade any aberrantly processed mRNAs in the nucleus. The exosome complex has been implicated in the biogenesis pathway of general messenger RNAs through its interaction with the 3′-end processing machinery. During the cell cycle, yeast histone mRNAs accumulate in the S-phase and are rapidly degraded as cells enter the G2-phase. To determine if the exosome contributes to the cyclic turnover of yeast histone mRNAs, we examined the pattern of accumulation of 'HTB1' mRNA during the cell cycle in a deletion strain of 'RRP6', a component of the nuclear exosome. Our results show that cells lacking Rrp6p continue to accumulate HTB1 mRNA as the cell cycle proceeds. This continued accumulation appears to result from a delay in exit from S-phase in *rrp6* cells. The accumulation of HTB1 mRNA in *rrp6* cells is influenced by the interaction of the nuclear exosome with the 3′-end processing machinery although there is no evidence for differential regulation of histone mRNA 3′-end processing during the yeast cell cycle.

INTRODUCTION

Histones are a highly conserved group of DNA-binding proteins required for the condensation of DNA in the eukaryotic nucleus. Coordinated regulation is required to ensure stoichiometric *de novo* production of the core histones in a time frame within the cell cycle coincident with DNA replication. The majority of histones are therefore regulated in a cell cycle manner and are termed replication-dependent histones (1,2). During S-phase of the cell cycle there is an accumulation of histone mRNAs, which are then rapidly degraded upon entry into G2. Regulation of histone mRNA levels results from control of histone gene transcription, mRNA 3′-end formation and mRNA degradation (3–5).

In higher eukaryotes, replication-dependent histone mRNAs are non-polyadenylated and the formation of the 3′-ends of the mRNAs contributes to their accumulation during the S-phase of the cell cycle. The 3′-ends of the mRNAs are defined by a highly conserved stem-loop (S-L) structure (6) and a loosely defined purine-rich element (7) that lie immediately upstream and downstream of the 3′-end cleavage sites, respectively. A number of proteins including a stem-loop-binding protein (SLBP) (8,9) and a 3′ to 5′ exonuclease (h3′exo) (10) interact with the S-L structure while the U7 snRNP interacts with the downstream element (11). Communication between the S-L and the downstream element is mediated by a zinc-finger protein (12). Recent studies have revealed that components of the general mRNA 3′-end cleavage and polyadenylation machinery are also required for metazoan histone mRNA 3′-end processing (13,14). The latter finding provides the first indication that common molecular machinery is involved in the processing of both polyadenylated and non-polyadenylated mRNAs.

Histone mRNA biogenesis is also cell cycle regulated in lower eukaryotes, such as fungi and protozoans, however, here the 3′-ends of histone mRNAs are polyadenylated (2,15,16). Both transcription and post-transcription events contribute to the accumulation of histone mRNAs in S-phase (17,18). Currently, little is known regarding the contribution of the individual steps in mRNA biogenesis towards the cell cycle accumulation pattern of histone mRNAs in lower eukaryotes. In a previous study, we have

*To whom correspondence should be addressed. Tel: +353 1 896 2578; Fax: +353 679 9294; Email: ubond@tcd.ie

identified a purine-rich region, termed the distal downstream element (DDE), which lies ~100 nt downstream of the 3′-end cleavage sites for the H2B-encoding mRNA, HTB1. Using a cell cycle-regulated chimera gene, neo-HTB1 (18), which contains the 3′ UTR, 3′-end cleavage sites and downstream sequences of the HTB1 gene fused to an open reading frame of a neomycin phosphotransferase gene, we showed that mutations in the DDE appear to prevent the cell cycle-dependent degradation of neo-HTB1, leading to its accumulation in G2-phase of the cell cycle. (19). The location of the DDE suggested that aberrant transcription termination might contribute to this effect although it is not clear how this could lead to transcript accumulation during the cell cycle.

It has been known for sometime that the process of mRNA 3′-end cleavage and polyadenylation is tightly coupled to transcription termination (20–24). Mutations in signal sequences on the primary transcript that control 3′-end cleavage and polyadenylation can reduce transcription termination efficiency (25). Conversely, null mutations in genes coding for certain cleavage/polyadenylation factors including the components of cleavage factor IA (CFIA), Rna14p, Rna15p and Pcf11p, result in the disruption of both 3′-end processing and transcription termination (25) leading to the accumulation of unprocessed read-through transcripts. These unprocessed transcripts are substrates for the nuclear exosome, a multi-subunit complex of 3′ to 5′ exonucleases (26), which rapidly degrades the transcripts in a process referred to as nuclear surveillance (27). Surprisingly, if the nuclear exosome component Rrp6p is deleted in a strain that also has inactive Rna14p or Rna15p, functional mRNAs can be produced from unprocessed 'read-through' transcripts by a 'chewing back mechanism' mediated by the core exosome, followed by polyadenylation (26). This observation has led to suggestions that this redundant function of the nuclear exosome may play a physiological role in regulating the abundance of specific mRNAs under certain conditions. There is evidence to show that the nuclear exosome component Rrp6 is required for the degradation of normal mRNAs that are retained in the nucleus (28) and for the autoregulation of specific mRNAs such as Nab2 and Nrd1 (29,30).

In addition to its role in nuclear surveillance, the nuclear exosome is required for the processing of many stable and unstable RNAs in the nucleus such as rRNAs, snoRNAs and snRNAs (31). Processing and/or degradation of these pre-RNAs requires an initial polyadenylation of the substrates, mediated by a complex consisting of the PolyA polymerases Trf4 and Trf5, the putative ATP-dependent RNA helicase, Mtr4p/Dob1p and zinc knuckle-binding proteins, Air1/2p, referred to as TRAMP. The polyadenylated substrates are subsequently degraded by the nuclear exosome. Recently, Reis and Campbell (32) have shown that loss of Trf4/5p or Rrp6p results in elevated levels of histone mRNAs in *Saccharomyces cerevisiae* suggesting that this may be a preferred pathway for histone mRNA degradation.

To further explore the links between 3′-end processing, transcription termination and the nuclear exosome in regulating histone mRNAs levels, we have examined the role of a number of RNA processing factors and the unique component of the nuclear exosome, Rrp6p, in the biogenesis of histone mRNAs. Our results show that the components of CFIA, Rna14p, Rna15p and Pcf11p are required for the 3′-end cleavage and proper termination of HTB1 mRNA and in the *rna14*/Δ*rrp6* double mutant, steady-state levels of functional polyadenylated HTB1 mRNA are restored to near wild-type levels. Furthermore, in the absence of Rrp6p (Δ*rrp6*), the normal pattern of HTB1 mRNA accumulation in the S-phase is disrupted. Flow cytometry analysis indicates that deletion of *rrp6* leads to a prolonged S-phase and this leads to HTB1 mRNA accumulation. The continued accumulation of HTB1 mRNA in *rrp6* cells is influenced by the interaction of the nuclear exosome with the 3′-end processing machinery. We propose a model to explain the role of the nuclear exosome in the cell cycle regulation of histone mRNAs.

MATERIALS AND METHODS

Yeast strains and growth conditions

Saccharomyces cerevisiae strains used in this study are listed in Table 1. Yeast strains were cultured at 22°C or 30°C in YEP (1% and 2% (w/v) yeast extract and bactopeptone, respectively), containing either 2% dextrose (YEPD) or 2% galactose (YEPGal) to an optical density at 660 nm (OD_{660}) of between 0.6 and 2.0. Plasmids containing a URA3 gene were introduced into yeast strains by the lithium acetate procedure as previously described (33). The transformants were selected on synthetic complete (SC) agar medium without uracil.

Table 1. Strains used in this study

Strain	Genotype	Source
S150	MAT**a**, *leu2-3_112, ura3-52, trp1-289, his3Δ*	Ref. (19)
W303A	MAT**a**, *leu2-3_112, ura3-52, trp1Δ2, his3-11, ade2-1, can1-100*	Euroscarf
W303B	MAT**a**, *leu2-3_112, ura3-1, trp1-1, his3-11_15, ade2-1, can1-100*	Ref. (34)
pcf11-2	MAT**a**, *leu2-3_112, ura3-1, trpΔ2, his3-11_15, ade2-1, pcf11-2*	Ref. (25)
rna14-3	MATα, *leu2-3_112, ura3-1, trp1-1, his3-11_15, ade2-1 can1-100, rna14-3,*	Ref. (34)
rna15-2	MAT**a**, *leu2-3_112, ura3-1, trp1-1, his3-11_15, ade2-1 can1-100, rna15-2,*	Ref. (34)
rrp6KO	MAT**a**, *leu2-3_112, ura3-1, trp1-1, his3-11-15, ade2-1, can1-100, rrp6::KAN*	Ref. (34)
rna14-3/Δrrp6	MAT**a**, *leu2-3_112, ura3-1, trp1-1, his3-11_15, ade2-1, can1-100, rna14-3, rrp6::KAN*	Ref. (34)
rna15-2/Δrrp6	MAT**a**, *leu2-3_112, ura3-1, trp1-1, his3-11_15, ade2-1, can1-100, rna15-2, rrp6::KAN*	Ref. (34)

For neomycin phosphotransferase expression, cells were plated on YEPGal plates containing 200 μg/ml G418.

Synchronization of yeast cells

Strains were grown in YEPD medium to early log phase. α_1-mating factor was added (final concentration of 2 μg/ml) and the culture was incubated for 3 h at 30°C or overnight at 22°C as indicated in figure legends 3 and 4 respectively. Cell cycle arrest was monitored by microscopic examination of the culture. When 90% of the cells were in G1-phase, they were collected by centrifugation and washed twice with sterile water. The pellets were resuspended in 200 ml of pre-warmed YEPD media and incubated at the temperatures indicated in the figure legends. For the temperature-sensitive strains, cells were incubated at either permissive (22°C) or non-permissive (37°C) temperatures for 1 h after α_1-mating factor removal. Samples were collected at 10 min or hour intervals and the cell pellets were frozen at −70°C until needed.

Flow cytometry analysis of cell cycle progression

Cells were synchronized with α_1-mating factor as described above. Cell samples were collected at 15 min intervals after removal of α_1-mating factor, fixed in 70% ethanol and stored at 4°C. The samples were washed in water and resuspended in 50 mM sodium citrate, pH 7.0. The cells were sonicated for 10 s at a setting of 5 amplitude microns on a SoniPrep sonicator (MSE). RNase A in 50 mM sodium citrate was added to give a final concentration of 0.1 mg/ml and the cells were incubated at 50°C for 2 h. Proteinase K was added to give a final concentration of 1 mg/ml and the cells incubated for a further 2 h at 50°C. Propidium iodide was added to give a final concentration of 4 μg/ml. Cell sorting as carried out on a Beckman Coulter Exics XL FACs Analysis machine. The data was analysed using Beckman Coutler Expo 32 ADC software.

RNA extraction and northern blot hybridization

RNA extractions, northern blotting and hybridizations were carried out as previously described (19) but using a slightly modified hybridization buffer [7% sodium dodecyl sulphate (SDS), 2% casein, 0.75 M NaCl, 0.075 M sodium citrate, 50 mM sodium phosphate (pH 7.0) and 0.1% *N*-lauroylsarcosine] at 68°C for 15–20 h Digoxigenin-dUTP (dig-dUTP) labelled DNA hybridization probes were prepared as described previously (19). Details of primers are listed in Table 2. An alkaline phosphate tagged anti-dig antibody and the CDP-star substrate were used according to manufacturer's instructions for detection of the hybridized probe.

Quantification of mRNA transcripts

Autoradiographs of northern blots were quantified using the densitometry software (Quantity One, version 4.2.1, Bio-Rad, Richmond, CA, USA). To account for variations in sample loading, the following normalization protocol was adopted. For cell cycle experiments, the 30 min time point following release from α-factor synchronization was used as a reference point (relative value = 1.0) for each probe. The value for each other time point was divided by this reference value to generate a normalized value. The normalized value for each of the time points for endogenous HTB1 was then divided by the corresponding normalized values for actin.

Reverse transcriptase reactions

To remove any contaminating DNA, RNA samples (30 μg) were incubated at 30°C for 1 h with RQ DNase (Promega Inc., Madison, WI, USA) according to supplier's instructions. Following digestion, the RNA was purified by adsorbing to silica columns (Sigma Chemical Co., Poole, UK). Reverse transcription reactions (20 μl) were carried out using 2 μg of DNAse-treated RNA as template, a transcript-specific reverse primer and reverse transcriptase (ImProm-II; Promega Inc., WI, USA) as specified by the manufacturer at 42°C for 60 min, followed by 15 min at 70°C. The PCR (25 μl) was carried out using 2 μl of cDNA and Taq polymerase (New England Biolabs, MA, USA) according to manufacturer's instructions. The primers used for cDNA synthesis are shown in Table 2 and in the figure legends. The cDNA was amplified using 25 cycles of (95°C for 30 s 55°C for 1 min and 72°C for 45 s) followed by final extension step was at 72°C for 7 min.

Real-time quantitative PCR

Real-time quantitative PCR was performed on Rotor-gene RG-3000 (Corbett Research, Canberra, AU) using Green Jumpstart ready mix as described by the manufacturer (Sigma Chemical) in 14 μl reaction volume and 2 μl of template (reverse transcription reaction) using 10 pmol of primers (HTB1_Endo_F and HTB1_Endo_R for endogenous *HTB1* and Actin_F2 and Actin_R2 for actin, see Table 2) and an annealing temperature of 55°C. The C_T values obtained were normalized to that of actin as described in the section above.

Table 2. Oligonucleotides used in this study

Name	Sequence
Forward 1	GTCTCTGAAGGTACTAGAGCTG
Reverse1	GGCCGCGGATTAAACTATTATACAA
Reverse2	TAAGCGCATTCCCTCTATGAGAC
Reverse3	TTTCTGAGTCATTAATAAGCAACACTA
Reverse4	GAAGTTAATCACAACAGAGGGTT
Reverse5	TTTTATACGTGCGTATTCTATTGTTCA
Reverse6	TGAAGTGCAGCTGACGATC
HTB1_F	GAAAAGAAACCAGCCTCC
HTB1_R	GAGTAGAGGAAGAGTACTTGG
Actin_F	TAGATTTTTCACGCTTACTGC
Actin_R	GGCTGCAGGTCGACTCTAGA
Neo_F	TACCTGCCCATTCGACCACCAAGCG
Neo_R	GTCATTTCGAACCCCAGAGTCCCGCTC
HTB1_Endo_F	GGCGCATGTCTGCTAAAGCCGAAAAG
HTB1_Endo_R	GCGCTTCTTGTTATACGCAGCC
Actin_F(2)	CCGCCTGAATTAACAATGGATTCTGAGG
Actin_R(2)	CTCTCAATTCGTTGTAGAAGGT

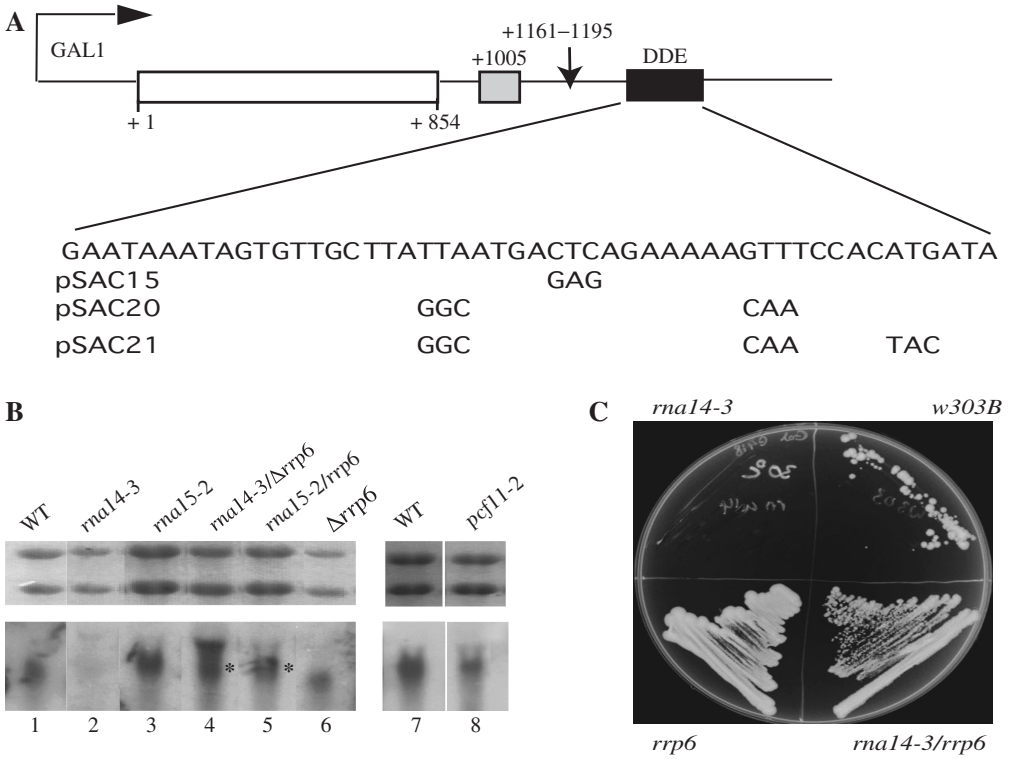

Figure 1. (**A**) Diagram of the structure of the neo-HTB1 chimeric gene. The gene is under the control of the GAL1 promoter. The HTB1 gene sequences (from nt position +1005) include the last 17 amino acids of the open reading frame (+1005 to +1062) (grey-shaded box), the 3′-UTR, 3′-end cleavage sites (arrow) and downstream sequences and are fused downstream of the neomycin phosphotransferase open reading frame (unshaded rectangle). The location of the DDE is indicated by a black box (+1276 to +1321). The sequences within the DDE are shown below the diagram and the sequence changes in pSAC 15, 20 and 21 are indicated below. (**B**) CFIA mutants affect the steady-state levels of neo-HTB1 mRNAs. The temperature-sensitive mutants *rna14-3*, *rna15-2* and *pcf11-2* were transformed with a plasmid containing the neo-HTB1 gene. RNA was extracted following incubation of the mutants for 1 h at the non-permissive temperature 37°C. Following electrophoresis and gel transfer, the neo-HTB1 mRNAs were detected using a digoxigenin-labelled DNA probe prepared using the primers neo_(F) and neo_(R), Table 2. The upper panel shows the 18S and 28S rRNAs used as a loading control. Note lane 3 is overloaded compared to the other lanes. Lane 1, 7: WT S. *cerevisiae* strain S-150B, 2: *rna14-3*, 3: *rna15-2*, 4: *rna14-3*/*Δrrp6*, 5: *rna15-2*/*Δrrp6*, 6: *Δrrp6*, 8: *pcf11-2*. *denotes processed mature mRNAs in lanes 4 and 5.(**C**) Growth of mutant strains on G418 plates. Mutant strains containing the neo-HTB1 plasmid were plated on YEPGal plates containing 200 μg/ml G418. Plates were incubated at 30°C.

RESULTS

3′-End processing of histone mRNAs is mediated by CFIA

Unlike in the higher eukaryotes, the mechanism of 3′-end processing of the polyadenylated histone mRNAs in lower eukaryotes has remained relatively unexplored. Since histone mRNAs can be correctly cleaved and polyadenylated in crude yeast whole cell extracts, it has been assumed that 3′-end processing is mediated by the general cleavage and polyadenylation machinery.

To test this assumption, the production of the GAL1 inducible chimeric neo-HTB1 mRNA (18,19), which contains the coding region of the neomycin phosphotransferase gene fused to sequences for the last 17 amino acids and the downstream 1300 nt of the HTB1 gene including the 3′-end cleavage sites, was examined in the CFIA temperature-sensitive mutants *rna14*, *rna15* and *pcf11* (Figure 1A) (34).

As shown in Figure 1B, accumulation of neo-HTB1 mRNA is significantly reduced at the non-permissive temperature in the mutants *rna14* (lane 2) and *pcf11* (lane 8) and to a lesser extent in *rna15* (lane 3). The reduction in steady-state levels of mRNAs is consistent with the known phenotype of CFIA mutants and reflects the rapid turnover of unprocessed transcripts by the nuclear exosome (26,35). Steady-state levels are partially restored when Rrp6p, a component of the nuclear exosome is also deleted in the *rna14* (Figure 1B, lane 4) and correctly sized mature WT neo-HTB1 transcripts are now apparent (Figure 1B, lane 4*). The neo-HTB1 transcripts produced in the *rrp6* and *rna14*/*rrp* strains are exported and can produce a functional neomycin phosphotransferase protein as observed by the growth on G418 plates, while under the same conditions, no functional protein is produced in *rna14* cells (Figure 1C). Interestingly, compared to its WT isogenic strain W303B (Table 1), more functional protein is expressed in *rna14*/*rrp6* and *rrp6* cells (Figure 1C). This reflects the general instability of neo-HTB1 in a number of WT strains of *S. cerevisiae* at temperatures greater than 30°C (Canavan,R., unpublished data). While neo-HTB1 mRNA levels are less affected by mutations in *rna15* (Figure IB, lane 3), more functional mRNA is produced in *rna15*/*rrp6* cells at the non-permissive temperature as indicated by growth on G418 plates (data not shown).

Mutations in the DDE alter the steady-state levels of neo-HTB1 mRNA in Δ*rrp6* cells

Previous work from our laboratory (19) has shown that mutations in a region lying ~100 nt downstream of the 3′-end cleavage sites of the HTB1 gene, termed the DDE, can influence the steady-state levels of the neo-HTB1 mRNA in asynchronous cells as well as during the cell cycle. Specifically, we previously observed that levels of neo-HTB1 mRNA were reduced in asynchronous cells in the mutant pSAC20 while its accumulation pattern during the cell cycle is altered in mutant pSAC21 (see Figure 1A for mutated bases). The steady-state levels of neo-HTB1 were unchanged in the mutant pSAC15 in asynchronous cells (Campbell and Bond, unpublished data). *In vitro* transcription run off studies revealed that the DDE lies in the region where transcription termination occurs (19). This led us to speculate that the DDE region may influence the steady-state levels of neo-HTB1 mRNA through its interaction with the 3′-end processing machinery. To examine this possibility, the levels of the mutant neo-HTB1 mRNAs transcribed from the mutants pSAC20, pSAC21 and pSAC15 were examined in the single mutants *rna14*-3 and *Δrrp6* and in the double mutant *rna14-3*/Δ*rrp6*. As shown in Figure 2A (lanes 1—4), the steady-state levels of DDE mutant neo-HTB1 mRNAs are somewhat reduced at the permissive temperature in *rna14-3* cells when compared to the levels of the WT neo-HTB1 mRNA. In the *rna14-3*/*Δrrp6* double mutant, the neo-HTB1 mRNA levels are restored (Figure 2A, lanes 5–8). In the single mutant *Δrrp6*, the DDE-mutant neo-HTB1 mRNAs appear to be preferentially stabilized relative to the WT neo-HTB1 mRNA (Figure 2A, lanes 9–12). At the non-permissive temperature, the levels of the WT and the mutant neo-HTB1 mRNAs are reduced in *rna14-3* cells (Figure 2B, lanes 1–4). The DDE mutant neo-HTB1 mRNAs appear more stable than the WT neo-HTB1 mRNA in the *Δrrp6* mutant background, although it should be noted that the WT neo-HTB1 RNA sample is under loaded (Figure 2B, lanes 9–12). Additionally, we noted that the steady-state levels of the WT and DDE mutant neo-HTB1 mRNAs could be influenced by the physiological state of the cells (our unpublished data). Taken together, the data indicates that neo-HTB1 mRNAs containing mutations in the DDE appear to be more unstable under conditions where 3′-end processing is inhibited but are stabilized in *Δrrp6* cells.

The nuclear exosome contributes to the accumulation and turnover of HTB1 mRNA during the cell cycle

We next questioned if the nuclear exosome may be contributing to the cell cycle regulation of endogenous histone mRNAs. The pattern of accumulation of the endogenous HTB1 mRNA was examined in WT and *Δrrp6* mutant cells. As shown in Figure 3A, the steady-state levels of the endogenous HTB1 mRNA steadily increase and peak between 60 and 70 min following removal of α-factor and rapidly decrease thereafter. Quantification of the northern blots and by real-time RT-PCR, reveals 4- to 5-fold increase in the steady-state levels of endogenous HTB1 transcript between time 0 and 70 min followed by rapid turnover of the RNA with levels returning to baseline by 110 min (Figure 3C). In the △*rrp6* background, the endogenous HTB1 mRNA appears to accumulate up to 50 min in a manner similar to that observed in the WT strain, however, thereafter, the RNAs levels decrease slightly and remain at the same level for the remainder of the time course (Figure 3B and C).

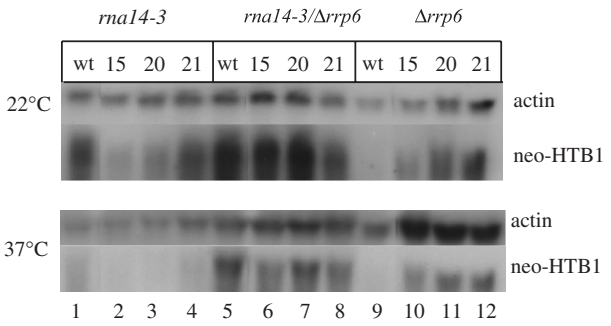

Figure 2. DDE mutants are preferentially unstable in *rna14*-3 and stabilized in *Δrrp6* cells. Strains *rna14*-3, *rna14*-3/*Δrrp6* and *Δrrp6* were transformed with plasmids containing the WT neo-HTB1 gene or the DDE mutant genes pSAC15, pSAC 20 or pSAC 21. Cells were incubated at the permissive temperature and prior to harvesting, were incubated at 22°C or 37°C for 1 h. RNA was extracted and probed for neo-HTB1 and actin mRNAs. Lanes 1, 5, 9: WT neo-HTB1, Lanes 2, 6, 10: pSAC 15 neo-HTB1, Lanes 3, 7, 11: pSAC 20. Lanes, 4, 8, 12: pSAC 21. Note lane 9 in the 22°C and 37°C panels is under loaded.

The observed difference in the accumulation of HTB1 in the WT and *rrp6* cells may reflect difference in the growth and division rate of the cells. As shown in Figure 3D, both the WT and *rrp6* mutant show very similar growth rate patterns and display a doubling time of ~3.3 and 3.4 h, respectively at 30°C. To examine the cell cycle progression in more detail, flow cytometry analysis of cells released following α-factor synchronization was preformed. As shown in Figure 3E, W303 and *rrp6* cells enter S-phase at the same rate. Cells with a 2*n* content appear at ~60 min after release from α-factor, which coincides with the peak in HTB1 mRNA levels. However, there is a slight delay in exit from S-phase in the *rrp6* cells. This delay in exit from S-phase may account for the continued accumulation of HTB1 mRNA in these cells. Taken together, the data suggests that the nuclear exosome Rrp6 contributes to S-phase accumulation of HTB1 mRNA and appears to alter the exit from S-phase.

Rrp6p influences HTB1 mRNA levels through its interaction with the 3′-end processing machinery but not as a result of differential 3′-end processing during the cell cycle

The nuclear exosome is known to play a role in degrading unprocessed and/or read-through transcripts in the nuclear surveillance pathway as demonstrated in Figure 1. Therefore the possibility arises that the 3′-end processing of histone mRNAs is differentially regulated during the cell cycle leading to an accumulation of unprocessed transcripts in the G_2-phase and thus generating substrates for the nuclear exosome. To test this hypothesis, the endogenous HTB1 mRNA levels were

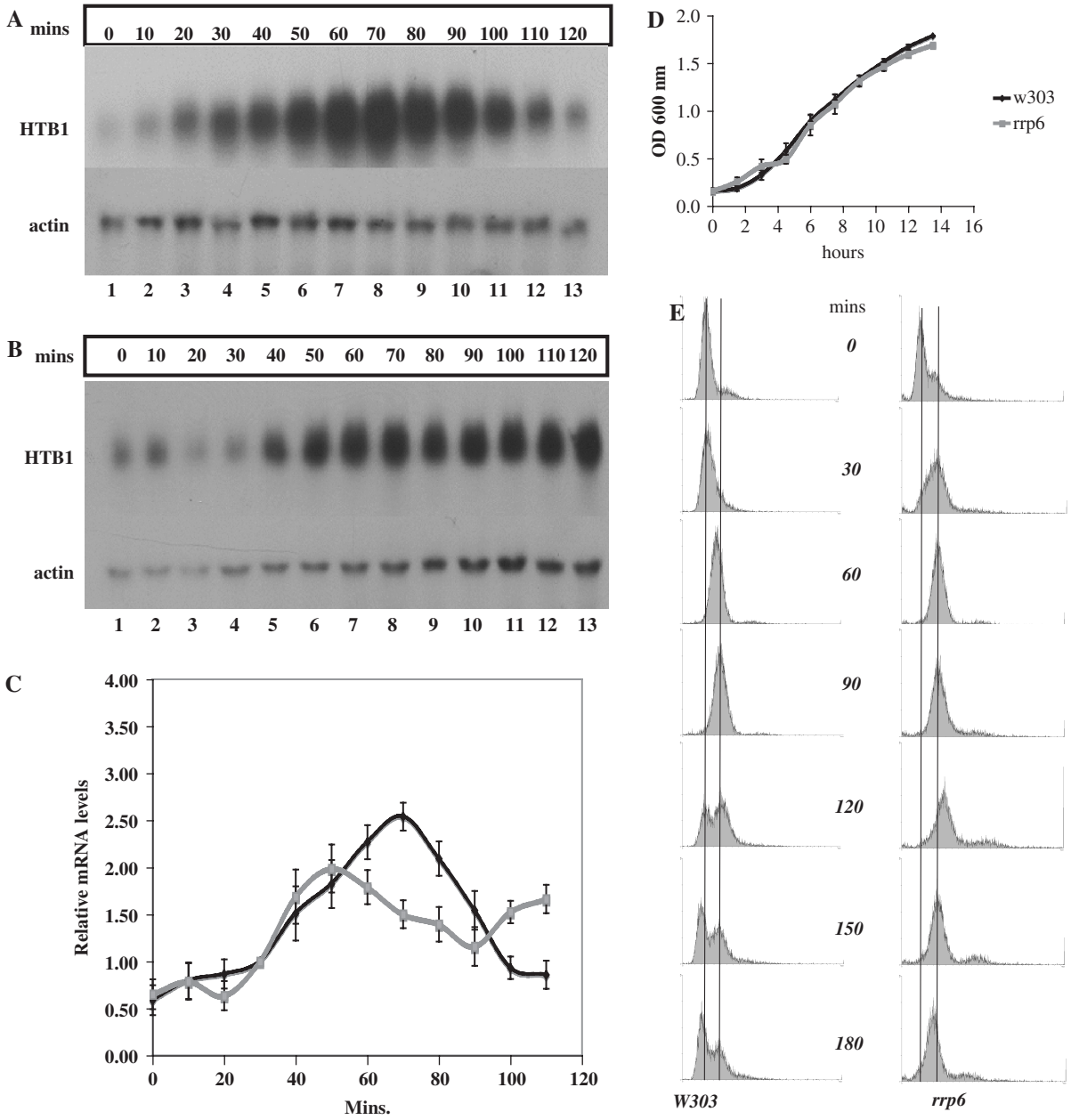

Figure 3. Deletion of RRP6 decreases the turnover of HTB1 mRNA following the S-phase of the cell cycle. Yeast strains W303A (**A**) and *Δrrp6* (**B**) were treated with α-factor as described in the Materials and Methods section. Samples were taken at 10-min intervals following removal of the α-factor. The extracted RNA was electrophoresed on a denaturing gel and transferred to a nylon membrane. The HTB1 and actin mRNAs were detected as described in the Materials and Methods section. (**C**) Quantification of HTB1 mRNA levels during the cell cycle. Normalized levels of *HTB1* mRNA in strains W303A (black line) and *Δrrp6* (grey line) following removal of α-factor. The data shown are the average levels obtained from real-time RT-PCR and northern blot analysis of four independent cell cycle experiments. The error bars represent the SE between experiments. The primers used for real time RT-PCR amplification of HTB1 and actin mRNAs are HTB1_Endo_F/HTB1_Endo_R and actin_F(2)/actin_R(2), Table 2. (**D**) Growth curve of W303 and *Δrrp6* at 30°C. Error bars represent the average error of triplicate reading of optical density at 600 nm. Black line, W303, grey line *Δrrp6*. (**E**) Flow cytometry analysis of synchronized W303 and *Δrrp6* cells. Cells were synchronized as described in the Materials and Methods section and samples taken every 15 min after α-factor removal. The cells were stained with propidium iodide and sorted as described in the Materials and Methods section. Flow analysis for every second sample is shown. Vertical lines show the position of 1*n* and 2*n* cells.

examined during the cell cycle in the *rna14-3/Δrrp6* mutant.

The cell cycle accumulation pattern of HTB1 mRNA in *rna14/Δrrp6* and its isogenic parent W303 cells grown at 22°C is shown in Figure 4A. At this temperature, the doubling time in both strains is ~6–7 h (data not shown). HTB1 mRNA levels persist for a longer period, up to 4 h in the absence of Rrp6p (Figure 4A, compare lanes 10–14 with lanes 1–5, 22°C panel). Inactivation of Rna14p by incubation of cells at 37°C for 1 h after removal of α-factor leads to an even greater persistence of HTB1 mRNA with levels remaining high for the following 6 h

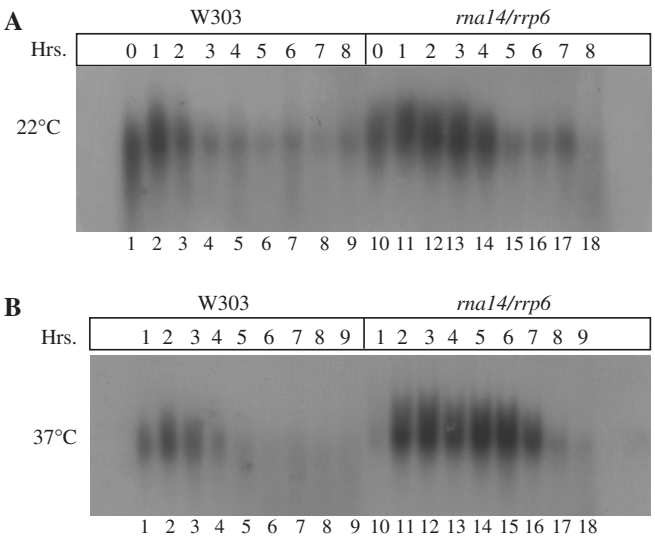

Figure 4. Cell cycle accumulation pattern of HTB1 mRNAs in *rna14-3/Δrrp6* cells. α-factor was added to strains W303B and *rna14-3/Δrrp6* and the cells were incubated overnight at 22°C. The α-factor was removed and cells were then incubated for a further hour at either 22°C or 37°C. The cells were then returned to 22°C for the remainder of the experiment. Samples were collected at 1 h intervals. HTB1 mRNA levels were detected as outlined in the Materials and Methods section. (**A**) Lanes 1–9, W303B incubated at 22°C, lanes 10–18, *rna14/Δrrp6* incubated at 22°C. (**B**) Lanes 1–9, W303B incubated at 37°C for 1 h after α-factor removal. Lane 1 sample was taken immediately after the 1 h incubation at 37°C. Lanes 10–18, *rna14-3/Δrrp6* incubated at 37°C for 1 h after α-factor removal. Lane 10 sample was taken immediately after the 1 h incubation at 37°C. The numbers above the figure show the time points after α-factor removal.

(Figure 4B, compare lanes 10–16 with lanes 1–7, 37°C panel). Thus, both Rrp6p and Rna14p appear to act in concert to influence the steady-state levels of HTB1 during the cell cycle.

To determine if 3′-end unprocessed transcripts, which might be potential substrates for the nuclear exosome, differentially accumulate during the cell cycle, reverse transcription reactions were carried out using a series of reverse primers corresponding to sequences immediately upstream or downstream of the 3′-end cleavage sites (Figure 5A), followed by PCR using a forward primer anchored in the 3′ UTR region of the HTB1 mRNA. In asynchronized *rna14-3/Δrrp6* cells grown at the permissive temperature, the majority of the transcripts correspond to correctly cleaved mRNAs (R1 primer) while some unprocessed transcripts are evident extending approximately to the region where the DDE lies (Figure 5B, 22°C, lanes 3–5). At the non-permissive temperature, we observe stabilized unprocessed pre-mRNA transcripts extending up to 450 nts beyond the 3′-end cleavage sites (Figure 5B, 37°C, lanes 2–7).

When the same primers were used in RT-PCR reactions using RNA isolated at 1 and 6 h following α factor release of W303 cells grown at 22°C (Figure 4), transcripts corresponding to correctly cleaved HTB1 (R1 primer) are evident at both time points (Figure 5C, 22°C panel lanes 3, 10*) and no read-through transcripts are apparent. Based on HTB1 accumulation patterns, these time points correspond to the S-phase and post S-phase of the cell cycle, respectively (Figure 4). Thus in WT cells, the majority of the transcripts are correctly cleaved in both the S-phase and the post-S-phase of the cell cycle. Products of the correct size were amplified by primers R1 and R2 in the 1 and 6 h samples of W303 cells that were treated at 37°C for 1 h after removal of α-factor (Figure 5C, 37°C panel, lanes 3, 4, 10, 11*). It should be pointed out that a number of artifactual bands are also evident in all lanes. This most likely reflects the relatively low levels of available substrate for cDNA synthesis using primers R2 through R6. Thus, preincubation of cells at 37°C in the first hour after α-factor release in of itself did not alter the 3′-end processing pattern of HTB1 mRNA during the cell cycle.

Similarly, the accumulation pattern of unprocessed read-through HTB1 transcripts was also examined in synchronized *rna14-3/Δrrp6* cells using RT-PCR. At the permissive temperature (22°C), only R1 and R2 primers can reverse prime and amplify products in samples taken 1 and 6 h after alpha factor release (Figure 5, panel D, 22°C, lanes 3, 4, and lanes 10, 11*). However, when the cells are shifted to the non-permissive temperature for 1 h after removal of α-factor to inactivate Rna14p, transcripts can now be amplified with the reverse primers R1, R2, R3 and R5 (Figure 5A) in both the 1 and 6 h samples (Figure 5D, 37°C panel, lanes 3–6, and lanes 10–13). Thus, the efficiency of 3′-end processing does not appear to vary significantly during the cell cycle and read-through unprocessed transcripts only accumulate under conditions when 3′-end processing is impaired (*rna14/Δrrp6* at 37°C, Figure 5D, 37°C panel).

DISCUSSION

The molecular mechanisms underlying the regulation of histone mRNA levels during the cell cycle in *S. cerevisiae* is poorly understood. In higher eukaryotes, the fluctuations in the steady-state levels of histone mRNAs during the cell cycle is mainly controlled by post-transcriptional events, specifically by mRNA 3′-end processing mediated by the interaction of unique protein factors with the conserved S-L structure at the 3′-end of the non-polyadenylated histone mRNAs and by the U7snRNP. Bioinformatic analysis of the yeast genome has not identified homologues of the SLBP nor the 3′ hExo both of which interact with the 3′-end of histone mRNAs in higher eukaryotes, nor have homologues of the U7 snRNP been identified (Bond,U., unpublished data). Since yeast histone mRNAs are polyadenylated but are cell cycle regulated, it appears that an alternative regulatory mechanism must have evolved to control the accumulation of histone mRNAs in the S-phase of the cell and their subsequent turnover in the G2-phase. Previous studies in *S. cerevisiae* have indicated that transcriptional regulation plays a major role in the accumulation patterns histone mRNAs during the cell cycle. Specifically, the transcriptional repressors Hir1p and Hir2p act coordinately to repress transcription in the G1-phase and through their ability to recruit components

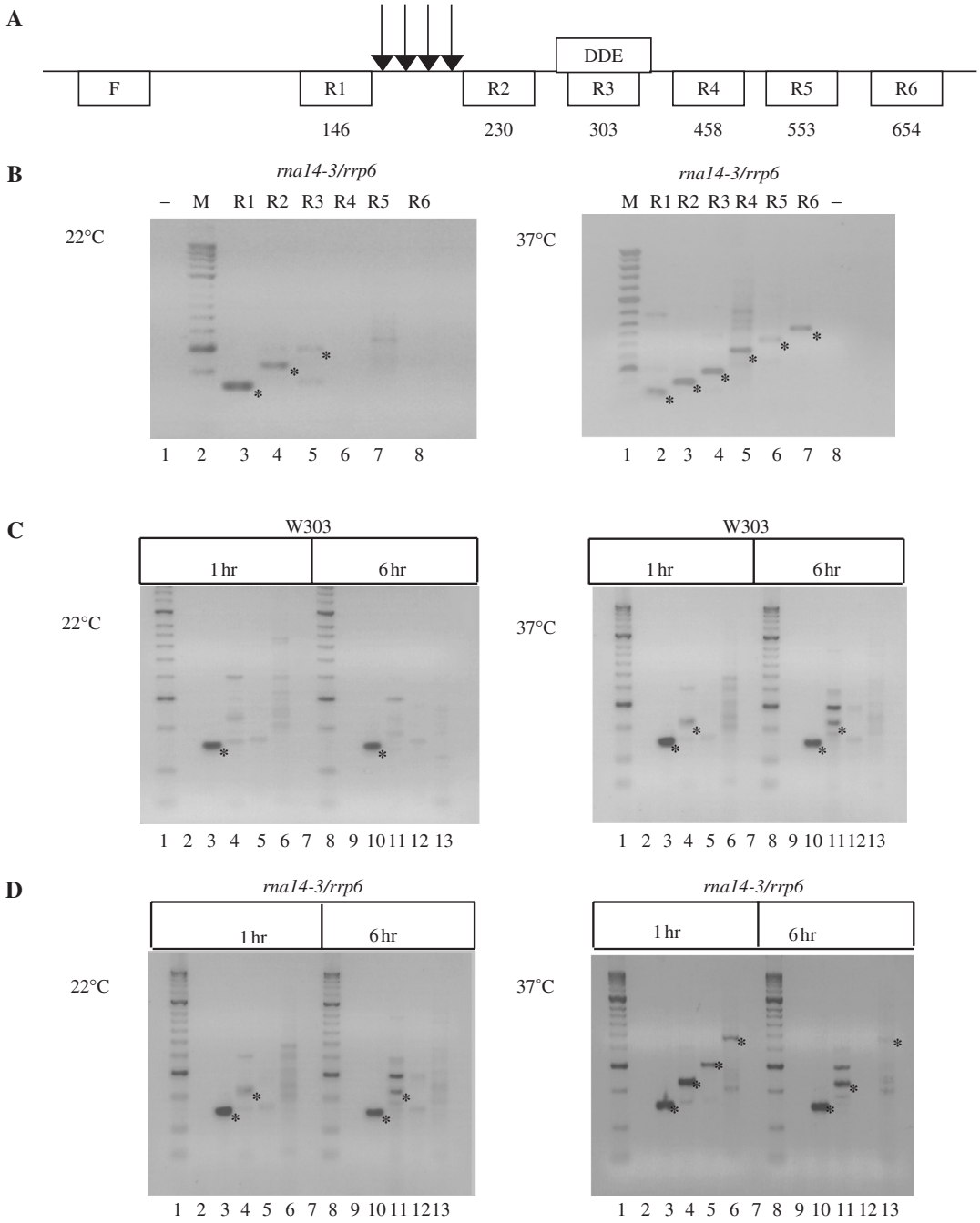

Figure 5. The 3′-ends of HTB1 mRNAs are not differentially processed during the cell cycle. (**A**) Diagram of the 3′-end of the *HTB1*. The location of the 3′-end cleavage sites (arrows) and the DDE are shown. The locations of the forward (F) and reverse (R) primers used for RT-PCR are shown. The expected sizes of the RT-PCR products using the common F primer and specific R primers are shown below each R primer. (**B**) RT-PCR products of HTB1 mRNA from *rna14-3*/*Δrrp6* cells grown at 22°C and then incubated for 1 h at either 22°C or 37°C prior to RNA extraction using the forward and reverse primers shown in A. Lane 1; F and R1 but no reverse transcriptase added. 2; DNA 100 bp ladder molecular weight marker, 3; primers F and R1, 4; primers F and R2, 5; primers F and R3, 6; primers F and R4, 7; primers F and R5, 8; primers F and R6. (**C**) RT-PCR products of W303 RNA extracted at 1 and 6 h following alpha factor release using the forward and reverse primers shown in A. Lanes 1, 8; DNA 100 bp ladder molecular weight marker. 2, 9; F and R1 but no reverse transcriptase added. 3, 10; primers F and R1. 4, 11; primers F and R2. 5, 12; F and R3. 6; 13; F and R5. (**D**) As for C but with RNA extracted from *rna14-3*/*Δrrp6* cells at 1 and 6 h following alpha factor release. *Note*: lane 12 is under loaded.

of the SWI/SNF chromatin-remodelling complex, activate expression in S-phase (2,36). Additionally, post-transcriptional events appear to contribute to the cell cycle regulation as chimera genes containing the 3′ untranslated region of the HTB1 gene can confer cell cycle periodicity to a neomycin phosphotransferase mRNA (18). The 5′ untranslated region appears to play a lesser role (17).

In this article, we have explored the mechanisms controlling histone mRNA 3′-end formation and cell cycle regulation in *S. cerevisiae*. Our analysis using the neo-HTB1 chimeric mRNA in CFIA mutants indicate that the 3′-ends of HTB1 mRNA are generated for the most part through the general 3′-end processing machinery. The steady-state levels of the neo-HTB1 mRNA transcripts are significantly reduced in the temperature-sensitive mutant *rna14*. Mutations in RNA15 (*rna15-2*), had a lesser impact on neo-HTB1 mRNA levels. This same phenotype was observed with a second mutant allele *rna15-1* (data not shown). The reduced effect of *rna15* mutants on HTB1 mRNA levels most likely reflects the fact that, in our hands, these temperature-sensitive mutants are not completely inactivated following heat treatment of the cells at 37°C: while cell growth is significanly reduced at this temperature, some growth is observed suggesting that these mutants only partially inactivate 3′-end processing. It is interesting to note that the differential effect of *rna14* and *rna15* mutants on the steady-state level of the neo-HTB1 transcripts was not noted in the analysis of other mRNA transcripts such as the Act1 or Cyc1 (26), although in this study the cells were incubated at 37°C for 2 h as opposed to the 1 h treatment used here. This may suggest that histone mRNAs show a lesser requirement for the Rna15p component of CF1A for 3′-end processing.

The neo-HTB1 primary transcripts are inherently unstable when 3′-end processing is inhibited, unlike actin mRNA transcripts which persist under these conditions (Figure 2). Deletion of *RRP6* in CFIA mutant backgrounds not only restores the levels of neo-HTB1 mRNA but also generates correctly sized transcripts representing fully processed mRNA. This RNA is exported from the nucleus and can be translated to produce functional proteins. Thus, even under conditions where 3′-end processing is inhibited, mature functional transcripts can be generated. Others have also observed similar 'processing' of read-through transcripts of a number of mRNAs in an *rna14*/*Δrrp6* background (26). It was postulated that these processed transcripts result from a trimming back of the read-through transcripts to the correct 3′-end by the 3′ to 5′ exonucleases of the core exosome and subsequent polyadenylation by Poly A Polymerase. An alternative hypothesis is that a sub-optimal 3′-end processing machine can now cleave and polyadenylate the unprocessed transcripts, which have been stabilized through a lack of action of Rrp6p. In either case, it appears that such redundant mechanisms exist to ensure that the production of key transcripts are generated despite adverse conditions. While the precise mechanism is not clearly understood, the data presented here verifies that Rrp6p appears to play a role in the biogenesis of histone mRNAs through its interaction with the 3′-end processing machinery.

Our results also show that the steady-state levels of neo-HTB1 mRNA appear to be influenced by the DDE sequence, which lies in the region of transcription termination of the HTB1 gene, specifically under conditions when 3′-end processing is inhibited or when RRP6 is deleted. Point mutations in the DDE region appears to reduce the stability of neo-HTB1 transcripts when the 3′-end processing is inhibited and conversely transcripts are more stable when RRP6 is deleted. This inverse relationship in mRNA stability in the two mutant backgrounds suggests that mutations in the DDE region of the HTB1 gene may alter the substrate specificity of the exosome thus allowing the mutant transcripts to escape degradation by the exosome or that some level of competition for binding to the DDE may occur between the 3′-end processing machinery and the nuclear exosome. The stability of the WT and DDE mutants can be influenced by the physiological conditions of the cell, particularly by cell density (our unpublished data). It is known that the 3′-end processing machinery communicates with RNA Polymerase II as it reaches the transcription termination site (23,25). It is possible that the DDE may act as a gateway for various 3′-end processing factors to access the transcription complex, thus establishing communication to effect transcription termination and subsequent processing.

The observation that the deletion of RRP6 alters the pattern of HTB1 transcript accumulation during the cell cycle provides an insight into a possible mechanism of histone mRNA regulation in *S. cerevisiae*. Quantification of HTB1 transcripts during the cell cycle by densitometry analysis of northern blots and quantitative real-time RT-PCR, indicates that while HTB1 mRNA levels appear to accumulate similarly in WT and Δ*rrp6* cells, thereafter, the levels decrease to baseline very quickly in the WT cells but in the Δ*rrp6* cells, HTB1 levels while decreasing slightly, persist throughout the remainder of the cell cycle. In fact, examination of HTB1 transcript levels in *rna14*/Δ*rrp6* at 22°C showed continued accumulation up to 4 h after alpha factor release, while in WT cells, levels return to baseline after 2 h The prolonged accumulation of HTB1 transcripts in Δ*rrp6* cells appears to be exacerbated by inactivation of 3′-end processing as HTB1 transcripts accumulate for an even longer time in the double mutant *rna14*/Δ*rrp6* at the non-permissive temperature.

Flow cytometry analysis of synchronized cells reveals that the prolonged accumulation of HTB1 in *rrp6* cells appears to result from a delay in exit of cells from S-phase or entry into M-phase. The reason for this delay in *rrp6* cells is currently unclear. Since RRP6 encodes for a 3′ to 5′ exonuclease, it is possible that Rrp6p is required for the decay of HTB1 mRNA at the end of S-phase and in the absence of this trigger, progression into M-phase is delayed. Alternatively, Rrp6p may regulate the levels of other mRNAs that encode for cell cycle checkpoint proteins. Interestingly, Gill *et al*. (37) have shown that accumulation of CLB2 mRNA, which encodes for B-cyclin, accounts for the exit from mitosis defect observed in RNase mitochondrial RNA processing (RNase MRP) mutants. The CLB2 mRNA was found to be a substrate for the RNase MRP endoribonuclease. Cleavage in the 5′ UTR region of CLB2 occurs at the end of mitosis, removing the 5′ cap and allows subsequent degradation by the 5′ to 3′ exonuclease Xrn1p. Thus, regulation of check point mRNAs at the level of mRNA stability may be a common theme in cell cycle regulation.

Recently Reis and Campbell (32) have identified a role for the nuclear poly (A) polymerases TRF4 and TRF5 complex in the regulation of bulk histone mRNA levels in yeast cells. Trf4/5p, together with Air1p, Air2p and Mtr4p, form the TRAMP complex, which has a specific function in the processing and/or degradation of rRNAs, snoRNAs and snRNAs. The TRAMP complex appears to 'tag' its substrates for processing and/or degradation by the nuclear exosome by adding a short polyA tail onto the 3′-end of these RNAs (31,38). Histone mRNA levels are elevated in Trf4/5 double mutants and likewise in strains bearing a deletion of *RRP6*, the HHF2 core histone transcript level was at least twice as much of the wild-type level. The level of HHF2 mRNA appears to come down at the end of S-phase but appears to have increased 4-fold in the subsequent S-phase. This is reminiscent of the suboptimal HTB1 transcript degradation we observed here. Taken together, the data provide clear proof for a role for the nuclear exosome in the regulation of histone mRNAs in yeast cells.

How might the nuclear exosome regulate histone mRNA levels during the cell cycle? Much of our understanding of how the nuclear exosome recognizes its intended targets comes from the analysis of its known substrates. First, the nuclear exosome is required for the 3′-end processing and transcription termination of snoRNAs and is recruited to the transcription termination sites via the RNA-binding proteins Nab3 and Nrd1 (38–43). Secondly, microarray analysis has revealed a small group of mRNAs whose steady-state levels are altered by deletion of RRP6. These include the autoregulated mRNAs Nrd1 and Nab2 (44). Thirdly, as shown previously and above, 3′-end unprocessed read-through transcripts are substrates for the nuclear exosome (26,27,45). A common theme among these exosome targets is the requirement for Nrd1/Nab3-binding sites. From the accumulated data, the model emerging is one in which the exosome complex is recruited to its substrate via its specific association with the RNA-binding protein Nrd1 (40). Substrates are then degraded in a 3′ to 5′ direction unless they encounter any additional Nrd1 recognition sites upstream which would block the progress of the exosome (39).

This model can also explain the 'processing' and subsequent polyadenylation of read-through unprocessed neo-HTB1 transcripts seen in *rna14/Δrrp6* strains. It is likely that this processing to a specific location reflects the presence of an Nrd1-binding site, which prevents further degradation by the exosome. In the presence of Rrp6p, complete degradation of the transcripts is observed suggesting that Rrp6p may add processivity to the core exosome or alternatively may prevent binding of Nrd1 to the transcript. It has been suggested that Nrd1 and the exosome may play a 'back-up' role in biogenesis of some mRNAs to ensure the production of mature mRNAs under certain conditions such as when the 3′-end processing machinery is inactivated (39). This suggests that the 3′-end processing machinery and the nuclear exosome may compete for the same pre-mRNA substrate and that physiological conditions in the cell will dictate the outcome of the competition. Extending this model, the data presented here suggests that HTB1 primary transcripts are recognized by the 3′-end processing machinery and the nuclear exosome in S-phase facilitating proper processing of the transcript. However, in G2-phase, the nuclear exosome interaction is favoured over the 3′-end processing machinery leading to an increase in the mRNA turnover. Whether this alteration in substrate specificity is due to changes in Nrd1 binding or alterations in 3′-end processing is currently unclear. However, our results showing that 3′-end processing is not differentially regulated during the cell cycle leads us to favour the former mechanism over the latter.

Thus, Rrp6 may contribute to histone mRNA biogenesis through its role in the nuclear surveillance pathway or through its interactions with the nuclear export pathways where it ensures that only correctly processed and functional mRNA can leave the nucleus (35). Alternatively, histone mRNAs may be retained in the nucleus in G2-phase thus evoking degradation of the transcripts by the DRN pathway (degradation of mRNA in the nucleus) (28). Rrp6p, along with nuclear cap-binding protein Cbc1p, has shown to be required for this pathway, which degrades mRNAs that are retained in the nucleus (46). It is interesting to note that the mammalian orthologue of RRP6, PM/Scl-100 (47), associates with the cytoplasmic exosome (48). Currently the role of the cytoplasmic mRNA degradation pathways (49) in the regulation of histone mRNAs has not been explored.

Finally, our finding that the nuclear exosome component Rrp6p contributes to the correct cell cycle accumulation pattern of HTB1 mRNA, acting in conjunction with transcriptional controls to contribute to the steady-state levels of histone mRNAs, provides further options to investigate the mechanisms controlling the regulation of histone mRNA during the yeast cell cycle.

ACKNOWLEDGEMENTS

We wish to thank T.C. James, Paul Beglan and Jane Usher for helpful advice and comments on the manuscript. We thank Tadgh O'Cronin for assistance with the Flow Cytometry. We thank Dr Nick Proudfoot and Dr Domenico Libri for yeast strains. This research was supported by grants SC/2002/081 and SC/2001/398 from Enterprise Ireland as part of the National Development Plan. Funding to pay the Open Access publication charges for this article was provided by a grant to U.B. from Science Foundation Ireland (Grant No. 06/RFP/GEN060).

Conflict of interest statement. None declared.

REFERENCES

1. Heintz,N. (1991) The regulation of histone gene expression during the cell cycle. *Biochim. Biophys. Acta*, **1088**, 327–339.
2. Osley,M.A. (1991) The regulation of histone synthesis in the cell cycle. *Annu. Rev. Biochem.*, **60**, 827–861.
3. Marzluff,W.F. and Duronio,R.J. (2002) Histone mRNA expression: multiple levels of cell cycle regulation and important developmental consequences. *Curr. Opin. Cell Biol.*, **14**, 692–699.

4. Marzluff,W.F. (2005) Metazoan replication-dependent histone mRNAs: a distinct set of RNA polymerase II transcripts. *Curr. Opin. Cell Biol.*, **17**, 274–280.
5. Kaygun,H. and Marzluff,W.F. (2005) Regulated degradation of replication-dependent histone mRNAs requires both ATR and Upf1. *Nat. Struct. Mol. Biol.*, **12**, 794–800.
6. Pandey,N.B., Williams,A.S., Sun,J.-H., Brown,V.D., Bond,U. and Marzluff,W.F. (1994) Point mutations in the stem-loop at the 3'end of mouse histone mRNA reduce expression by reducing the efficiency of 3'end formation. *Mol. Cell. Biol.*, **14**, 1709–1720.
7. Bond,U.M., Yario,T.A. and Steitz,J.A. (1991) Multiple processing-defective mutations in a mammalian histone pre-mRNA are suppressed by compensatory changes in U7 RNA both *in vivo* and *in vitro*. *Genes Dev.*, **5**, 1709–1722.
8. Wang,Z.F., Whitfield,M.L., Ingledue,T.C., Dominski,Z. and Marzluff,W.F. (1996) The protein that binds the 3' end of histone mRNA: a novel RNA-binding protein required for histonepre-mRNA processing. *Genes Dev.*, **10**, 3028–3040.
9. Martin,F., Schaller,A., Eglite,S., Schumperli,D. and Muller,B. (1997) The gene for histone RNA hairpin binding protein is located on human chromosome 4 and encodes a novel type of RNA binding protein. *EMBO J.*, **16**, 769–778.
10. Yang,X., Purdy,M., Marzluff,W. and Dominski,Z. (2006) Characterization of 3'hExo, a 3' exonuclease specifically interacting with the 3' end of histone mRNA. *J. Biol. Chem.*, **281**, 30447–30454.
11. Mowry,K.L. and Steitz,J.A. (1987) Identification of the human U7 snRNP as one of several factors involved in the 3' end maturation of histone premessengers RNAs. *Science*, **238**, 1682–1687.
12. Dominski,Z., Erkmann,J.A., Yang,X., Sanchez,R. and Marzluff,W.F. (2002) A novel zinc finger protein is associated with U7 snRNP and interacts with the stem–loop binding protein in the histone pre-mRNP to stimulate 3'-end processing. *Genes Dev.*, **16**, 58–71.
13. Dominski,Z., Yang,X. and Marzluff,W.F. (2005) The polyadenylation factor CPSF-73 is involved in histone-pre-mRNA processing. *Cell*, **123**, 37–48.
14. Kolev,N.G. and Steitz,J.A. (2005) Symplekin and multiple other polyadenylation factors participate in 3'-end maturation of histone mRNAs. *Genes Dev.*, **19**, 2583–2592.
15. Fahrner,K., Yarger,J. and Hereford,L. (1980) Yeast histone mRNA is polyadenylated. *Nucleic Acids Res.*, **8**, 5725–5737.
16. Puerta,C., Martin,J., Alonso,C. and Lopez,M.C. (1994) Isolation and characterization of the gene encoding histone H2A from *Trypanosoma cruzi*. *Mol. Biochem. Parasitol.*, **64**, 1–10.
17. Lycan,D.E., Osley,M. and Hereford,L.M. (1987) Role of transcriptional and post-transcriptional regulation in the expression of histone genes in *Saccharomyces cerevisiae*. *Mol. Cell. Biol.*, **7**, 614–621.
18. Xu,H., Johnson,L. and Grunstein,M. (1990) Coding and noncoding sequences at the 3' end of yeast histone H2B mRNA confer cell cycle regulation. *Mol. Cell. Biol.*, **10**, 2687–2694.
19. Campbell,S.G., Li Del Olmo,M., Beglan,P. and Bond,U. (2002) A sequence element downstream of the yeast HTB1 gene contributes to mRNA 3' processing and cell cycle regulation. *Mol. Cell. Biol.*, **22**, 8415–8425.
20. Minvielle-Sebastia,L. and Keller,W. (1999) mRNA polyadenylation and its coupling to other RNA processing reactions and to transcription. *Curr. Opin. Cell Biol.*, **11**, 352–357.
21. Proudfoot,N.J. (2000) Connecting transcription to messenger RNA processing. *Trends Biochem. Sci.*, **25**, 290–293.
22. Proudfoot,N.J., Furger,A. and Dye,M.J. (2002) Integrating mRNA processing with transcription. *Cell*, **108**, 501–512.
23. Buratowski,S. (2005) Connections between mRNA 3' end processing and transcription termination. *Curr. Opin. Cell Biol.*, **17**, 257–261.
24. Sadowski,M., Dichtl,B., Hubner,W. and Keller,W. (2003) Independent functions of yeast Pcf11p in pre-mRNA 3' end processing and in transcription termination. *EMBO J.*, **22**, 2167–2177.
25. Birse,C.E., Minvielle-Sebastia,L., Lee,B.A., Keller,K. and Proudfoot,N. (1998) Coupling transcriptional termination to messenger RNA maturation in yeast. *Science*, **280**, 298–301.
26. Torchet,C., Bousquet-Antonelli,C., Milligan,L., Thompson,E., Kufel,J. and Tollervey,D. (2002) Processing of 3'-extended read-through transcripts by the exosome can generate functional mRNAs. *Mol. Cell*, **9**, 1285–1296.
27. Milligan,L., Torchet,C., Allmang,C., Shipman,T. and Tollervey,D. (2005) A nuclear surveillance pathway for mRNAs with defective polyadenylation. *Mol. Cell. Biol.*, **25**, 9996–10004.
28. Das,B., Butler,J.S. and Sherman,F. (2003) Degradation of normal mRNA in the nucleus of *Saccharomyces cerevisiae*. *Mol. Cell. Biol.*, **20**, 2827–2838.
29. Roth,K.M., Wolf,M.K., Rossi,M. and Butler,J.S. (2005) The nuclear exosome contributes to autogenous control of NAB2 mRNA levels. *Mol. Cell. Biol.*, **25**, 1577–1585.
30. Arigo,J.T., Carroll,K.L., Ames,J.M. and Corden,J.L. (2006) Regulation of yeast NRD1 expression by premature transcription termination. *Mol. Cell*, **21**, 641–651.
31. LaCava,J., Houseley,J., Saveanu,C., Petfalski,E., Thompson,E., Jacquier,A. and Tollervey,D. (2005) RNA degradation by the exosome is promoted by a nuclear polyadenylation complex. *Cell*, **121**, 713–724.
32. Reis,C.C. and Campbell,J.L. (2006) Contribution of Trf4/5 and the nuclear exosome to genome stability through regulation of histone mRNA levels in *Saccharomyces cerevisiae*. *Genetics*, **175**, 993–1010.
33. Ito,H., Fukuda,Y., Murata,K. and Kimura,A. (1983) Transformation of intact yeast cells treated with alkali cations. *J. Bacteriol.*, **3**, 163–168.
34. Minvielle-Sebastia,L., Winsor,B., Bonneaud,N. and Lacroute,F. (1991) Mutations in the yeast RNA14 and RNA 15 genes result in an abnormal mRNA decay rate: sequence analysis reveals an RNA-binding domain in the RNA protein. *Mol. Cell. Biol.*, **11**, 3075–3087.
35. Libri,D., Dower,K., Boulay,J., Thomsen,R., Rosbash,M. and Jensen,T.H. (2002) Interactions between mRNA export commitment, 3'-end quality control, and nuclear degradation. *Mol. Cell. Biol.*, **22**, 8254–8266.
36. Spector,M.S., Raff,A., DeSilva,H., Lee,K. and Osley,M. (1997) Hir1p and hir2p function as transcriptional corepressors to regulate histone gene transcription in the Saccharomyces cerevisiae cell cycle. *Mol. Cell. Biol.*, **17**, 545–552.
37. Gill,T., Cai,T., Aulds,J., Wierzbicki,S. and Schmitt,M.E. (2004) RNase MRP cleaves the CLB2 mRNA to promote cell cycle progression: novel method of mRNA degradation. *Mol. Cell. Biol.*, **24**, 945–953.
38. Arigo,J.T., Eyler,D.E., Carroll,K.L. and Corden,J.L. (2006) Termination of cryptic unstable transcripts is directed by yeast RNA-binding proteins Nrd1 and Nab3. *Mol. Cell*, **23**, 841–851.
39. Kim,M., Vasiljeva,L., Rando,O.J., Zhelkovsky,A., Moore,C. and Buratowski,S. (2006) Distinct pathways for snoRNA and mRNA termination. *Mol. Cell*, **24**, 723–734.
40. Vasiljeva,L. and Buratowski,S. (2006) Nrd1 interacts with the nuclear exosome for 3' processing of RNA polymerase II transcripts. *Mol. Cell*, **21**, 239–248.
41. Carroll,K.L., Ghirlando,R., Ames,J.M. and Corden,J.L. (2007) Interaction of yeast RNA-binding proteins Nrd1 and Nab3 with RNA polymerase II terminator elements. *RNA*, **13**, 361–373.
42. Steinmetz,E.J., Ng,S.B., Cloute,J.P. and Brow,D.A. (2006) Cis- and trans-acting determinants of transcription termination by yeast RNA polymerase II. *Mol. Cell. Biol.*, **26**, 2688–2696.
43. Steinmetz,E.J. and Brow,D.A. (1998) Control of pre-mRNA accumulation by the essential yeast protein Nrd1 requires high-affinity transcript binding and a domain implicated in RNA polymerase II association. *Proc. Natl Acad. Sci. USA*, **95**, 6699–6704.
44. Houalla,R., Devaux,F., Fatica,A., Kufel,J., Barrass,D., Torchet,C. and Tollervey,D. (2006) Microarray detection of novel nuclear RNA substrates for the exosome. *Yeast*, **23**, 439–454.
45. Bousquet-Antonelli,C., Presutti,C. and Tollervey,D. (2000) Identification of a regulated pathway for nuclear pre-mRNA turnover. *Cell*, **102**, 765–775.

46. Kuai,L., Das,B. and Sherman,F. (2005) A nuclear degradation pathway controls the abundance of normal mRNAs in *Saccharomyces cerevisiae*. *Proc. Natl Acad. Sci. USA*, **102**, 13962–13967.
47. Briggs,M.W., Burkard,K.T. and Butler,J.S. (1998) Rrp6p, the yeast homologue of the human PM-Scl 100-kDa autoantigen, is essential for efficient 5.8 S rRNA 3' end formation. *J. Biol. Chem.*, **273**, 13255–13263.
48. van Dijk,E.L., Schilders,G. and Pruijn,G.J.M. (2007) Human cell growth requires a functional cytoplasmic exosome, which is involved in various mRNA decay pathways. *RNA*, **13**, 1027–1035.
49. Lejeune,F., Li,X. and Maqua,L.E. (2003) Nonsense-mediated mRNA decay in mammalian cells involves decapping, deadenylating, and exonucleolytic activities. *Mol. Cell*, **12**, 675–687.